

On situ vibration-based structural health monitoring of a railway steel truss bridge: a preliminary numerical study.

Lorenzo Bernardini, Claudio Somaschini, Andrea Collina



INFORMATION

Keywords:

Steel truss bridge
railway bridge
structural health monitoring
direct monitoring
vibration-based monitoring.

DOI: 10.23967/wccm-apcom.2022.088

Published: 06/07/2022

ON SITU VIBRATION-BASED STRUCTURAL HEALTH MONITORING OF A RAILWAY STEEL TRUSS BRIDGE: A PRELIMINARY NUMERICAL STUDY.

LORENZO BERNARDINI¹, CLAUDIO SOMASCHINI¹ AND ANDREA COLLINA¹

¹Department of Mechanical Engineering, Politecnico di Milano

Via G. La Masa 1, 20156

lorenzo.bernardini@polimi.it

claudio.somaschini@polimi.it

andrea.collina@polimi.it

Key words: Steel truss bridge, railway bridge, structural health monitoring, direct monitoring, vibration-based monitoring.

Abstract. *Railway network is subject to increasing travelling loads and traffic frequency. In addition, since most of the bridges were built in the last century, they are subject to ageing and degradation. It is therefore necessary to develop proper structural health monitoring systems that can support periodical visual inspections. In this context, direct monitoring systems represent an important and promising solution for structural health monitoring purposes. This paper is the result of a numerical study performed on a 3D FE bridge model based on an existing structure: the latter is a Warren truss railway bridge, located in Northern Italy, built few years after the end of the second world war. The purpose of the study is to numerically evaluate the effectiveness in damage detection and localization of different vibration-based techniques. This analysis has been performed for a set of different damage scenarios, suggested by the infrastructure managers.*

1 INTRODUCTION

Railway networks include also bridge and viaducts that can have a considerable age, namely more than 50 years, while they are getting older, at the same time they are subjected to increasing travelling loads and traffic frequency [1], which are combined with degradation and ageing over time. Some examples concerning railway network that have a long history dating back to 19th century, can be found in the literature.

In Japan, for example, 20% of existing steel bridges at year 2016, were older than 50 years (see [2]). In India too, that has a considerable extension of railway network, it is mentioned that there are over 37,000 railway bridges which are 100 years old. About 10% of these bridges have been repaired or strengthened during the 2012-2017 period. In Europe, the oldest bridges are masonry bridges, but also a considerable percentage (10%) of steel bridges with an age between 50 years and 100 can be found, and 5% are more than a century old ([3]). Most of the bridges in North America and Europe were built during the last century, before the 1970s [3],[5],[6].

The challenge for infrastructure managers is to ensure operation safety of such infrastructures that have a long service history: this is done through periodical inspections, carried out with increasing levels, as defects or damage are discovered by the first level of inspection.

The periodicity of the inspections depends on the type of the bridge (masonry, concrete, steel, etc.) and on its age, and can be supported, at higher levels of inspection, by several NDT techniques (see [8] for a general overview).

Complementary to the direct search of damage, the Structural Health Monitoring (HSM) is an approach based on the detection of defects analysing directly the dynamical response of the bridge placing sensors on it (direct approach [9], [10]), or of an instrumented vehicle running over a bridge (indirect [1], [11] approach).

This paper deals with direct approach, whose aim is to get a continuous and real-time assessment of the health status of the studied structure by using sensing devices positioned on the structure itself. To reach this goal, the choice of damage-sensitive indexes plays a key role. The data gathered in time by the transducers, once properly analysed, have the potential to highlight the sign of a damage occurring on the structure, through the comparison between standard (supposedly healthy) condition and its dynamical behaviour.

Vibration-based methods [12], [13] exploit structural vibrations, measured in different points, to extract features able to define the actual condition of the structure subject to the analysis.

This work consists of a numerical preliminary study on an existing truss railway bridge with the aim to investigate the effectiveness of two different vibration-based approaches for diagnostic purposes. Assuming damage scenarios affecting truss bridge cross-girders and lower chords, the first approach consisted in the evaluation of the changes in terms of modal parameters caused by the defect scenarios on the structure. In this regard, eigen frequencies and mode shapes were studied, processing the vibrational decay following train transit.

The second approach consists of the direct analysis of vibrational time histories evaluated in different points of the structure during the train transit. Comparing bridge vibrations under moving train loads with the healthy case, the idea is to investigate the possibility to detect damage presence and its indicative position.

A recent developed way is to process the data of the time series using machine learning to extract signature of the damage from data analysis ([9]). The cited paper works on a real truss bridge, out of the line in operation. The bridge is excited by dynamic actuators, to reproduce ambient excitations, while damages are inserted temporarily removing the bolts of the different connections.

In this paper an existing warren type bridge in service is studied, whose modal parameters have been identified from field analysis. A FEM model is developed from the modal parameters of the bridge and used for the simulation of train-bridge dynamical interaction. The healthy condition is assumed as the one found from the field dynamical identification, while several locations of damages are inserted once at a time, in the FEM model of the bridge.

The analysis of modal parameters modification and the direct response of the bridge during train transit are presented and compared. To this purpose, vehicle-bridge dynamic interaction was simulated considering an ETR500 by means of ADTreS software developed by researchers of Mechanical Engineering Department of Politecnico di Milano.

Concerning the processing of the vibrational time series during train transit, the paper

analyses also the impact of the geometrical track irregularity, that acts as a considerable disturbance on the comparison between healthy and damaged condition carried out on the direct time series of vibrational signals. To this purpose, simulations were performed with and without track irregularity: for the latter case, irregularity profiles recorded by diagnostic train on the real bridge were used. An analysis considering this issue was not found in the literature yet.

The paper is divided into the following sections: in section 2 the FEM model of the bridge is presented and validated by means of the comparison between numerical and experimental modal parameters (natural frequencies and mode shapes). Moreover, damage scenarios and the simulation pattern are presented. Section 3 is intended to show the impact of the studied damage scenarios on bridge eigen frequencies and mode shapes. Then, section 4 presents and discuss the results concerning the second vibration-based diagnostic approach. Finally, main conclusions are drawn, and future development are envisaged.

2 BRIDGE MODEL AND DEFECT SCENARIOS

The bridge considered in this work is a Warren steel truss bridge composed by seven modules and a closed cross-section, it is 5.2 m wide and 60.48 m long, with a height of 7.70 m, as shown in Figure 1. The bridge is located along a regional railway line in Veneto region, in Northern Italy, over Piave river. The track is without ballast, and the rails are connected to bridge deck through wooden sleeper, directly placed on the deck girder. The assembled 3D beam model was set up starting from original blueprints and technical drawings.

Table 1 collects the bridge's main eigenfrequencies; the numerical values obtained from the model are compared with the experimental values evaluated during an experimental field campaign carried out in October 2020. A mesh of six wireless accelerometers was used in order to evaluate experimental frequencies and associated mode shapes: the sensors were positioned according to Figure 1 (green points). The use of wireless accelerometers was chosen to minimize the installation set-up effort, the limited number of transducers was also adopted to verify what level of detection of defect could be reached with a limited number of sensors.

Table 1 shows a fair agreement between numerical and experimental values of natural frequencies. Maximum difference is around 4.25 %, for the lateral 1 mode, while for the modes that involve vertical motion the highest difference is 4.32 %.

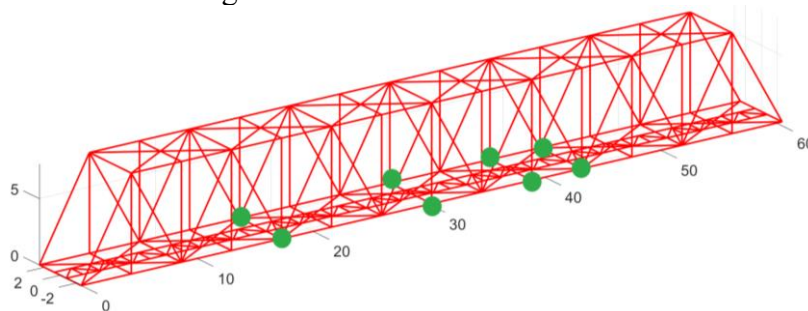


Figure 1: Bridge FEM model. Positions in which accelerometers were positioned during the experimental campaign (October 2020) are highlighted with green circles.

In Table 1, two distinct 1st lateral modes (i.e., A and B) can be observed, both featured by a minor vertical component. While the lateral component is very similar between these two modes, the vertical one is higher for mode B.

Table 1: First numerical and experimental frequencies.

| N. | Mode shape | Num. Freq. [Hz] | Exp. Freq. [Hz] | Difference % |
|----|---------------------------|-----------------|-----------------|--------------|
| 1 | 1 st Lateral A | 2.35 | 2.25 | 4.25 |
| 2 | 1 st Lateral B | 4.36 | 4.45 | 2.02 |
| 3 | 1 st Bending | 4.39 | 4.20 | 4.32 |
| 4 | 2 nd Lateral | 5.02 | 5.00 | 0.40 |

Next, numerical and experimental mode shapes are compared by means of computing MAC coefficients (see Eq.(1), where n is the number of sensor nodes): numerical mode shapes have been evaluated in the positions in which accelerometers were placed during the experimental campaign (see green circles in Figure 1), considering vertical and lateral direction:

$$MAC(A, X) = \frac{|\sum_{j=1}^n \psi_{x,j}^T \cdot \psi_{A,j}|^2}{(\sum_{j=1}^n \psi_{x,j}^T \cdot \psi_{x,j}) \cdot (\sum_{j=1}^n \psi_{A,j}^T \cdot \psi_{A,j})} \quad (1)$$

In (1) the experimental $\psi_{x,i}$ and numerical $\psi_{A,i}$ vertical and lateral components are used to evaluate MAC index. Figure 2 illustrates the resulting MAC matrix: in general, a good degree of similarity can be observed between numerical and experimental modes, considering a mesh of eight points, as shown in Figure 1, for a total of sixteen channels. This outcome is reflected by high diagonal values, that are all very close to 1. It is also possible to observe relatively high values in the extra-diagonal positions (1,2) and (2,1) respectively: this result is though to be rcaused by the similarity between the 1st lateral A and B mode shapes in correspondance of the limited number of measuring points.

The analysis of defects is subsequently carried out on the so validated FEM model. For what concerns the simulated damage, defects occurring at two bridge elements are modelled, with the following scenarios:

- **Damage A:** entrance right lower chord element;
- **Damage B:** seventh cross-girder from the bridge entrance;
- **Damage C:** second cross-girder from the bridge exit;
- **Damage D:** midspan lower chord elements;

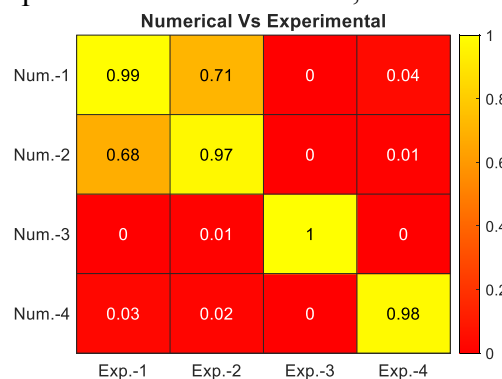


Figure 2: MAC matrix computed between numerical and experimental mode shapes.

The structural damage is modelled through a reduction of the 50% the Young modulus of the interested beam element: this affects both axial and flexural stiffness. The considered damage scenarios were suggested by the infrastructure manager.

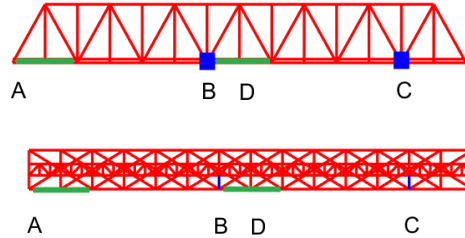


Figure 3: Investigated damage positions across the bridge span. Three different locations of the damage were considered, i.e. A, B and C.

3 MODAL PARAMETERS BASED METHOD

In this section the effects of the previously defined damage on bridge modal parameters in terms of eigenfrequencies and associated mode shapes are investigated. The computation, that was carried out for the healthy bridge leading to the results presented in section 2, had been repeated for all the three damage scenarios. Considering Table 2, it is possible to observe that no appreciable changes in terms of frequency have been obtained by the presence of the modelled damages, except for scenario D and the first bending frequency.

Table 2: Numerical bridge eigenfrequencies, in case of healthy structure, and damages A, B, C and D locations. The column Diff is related to damage scenario D.

| Mode | Healthy [Hz] | A [Hz] | B [Hz] | C [Hz] | D [Hz] | Diff. D/H% |
|---------------------------|--------------|--------|--------|--------|--------|------------|
| 1 Lateral 1 | 2.35 | 2.33 | 2.35 | 2.35 | 2.33 | 0.85 |
| 2 Lateral 2 | 4.36 | 4.36 | 4.36 | 4.36 | 4.36 | 0.00 |
| 3 1 st Bending | 4.39 | 4.38 | 4.39 | 4.39 | 4.33 | 1.36 |
| 4 Lateral 3 | 5.02 | 5.01 | 5.02 | 5.02 | 5.02 | 0.20 |

Beside the changes in the natural frequencies, alterations in the mode shapes due to damage occurrence were studied; to quantify these changes MAC index was used again (refer to Eq. (1)). In this case MAC is not evaluated for comparing numerical with experimental modes (as previously done), but, instead, it is computed considering numerical modes of healthy and damaged modelled structure respectively, in order to detect possible changes in mode shapes due to the presence of a damage. Considering a further reduced mesh of sensors, composed of six nodes instead of eight (green points, shown in Figure 4) the results in terms of MAC matrices are reported in Figure 5.

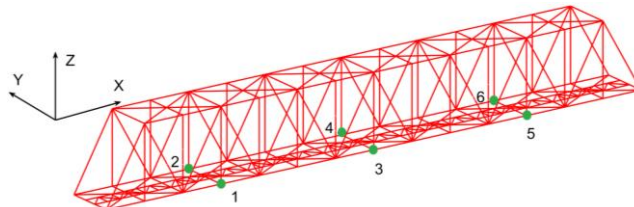


Figure 4: Sensors mesh assumed on the bridge deck. Green points (1-6) stand for points in which vertical displacement, velocity and acceleration signals are measured.

Most of the considered damage scenarios (see Figure 3) are not severe enough to produce detectable modifications in the bridge's mode shapes. Instead, damage scenario D results in a detectable change of the lateral 2 and bending mode shapes, despite a variation of the associated eigenfrequency below 1.5 %. Second and third mode related diagonal term reduces from unity to 0.75 and 0.68 respectively, in combination with an increase of the related off-diagonal terms, raising from zero (compare Figure 2) to 0.26 and 0.31 (see Figure 5d). Combining natural frequency and MAC analysis, it is therefore possible to detect the presence of a defect in the bridge.

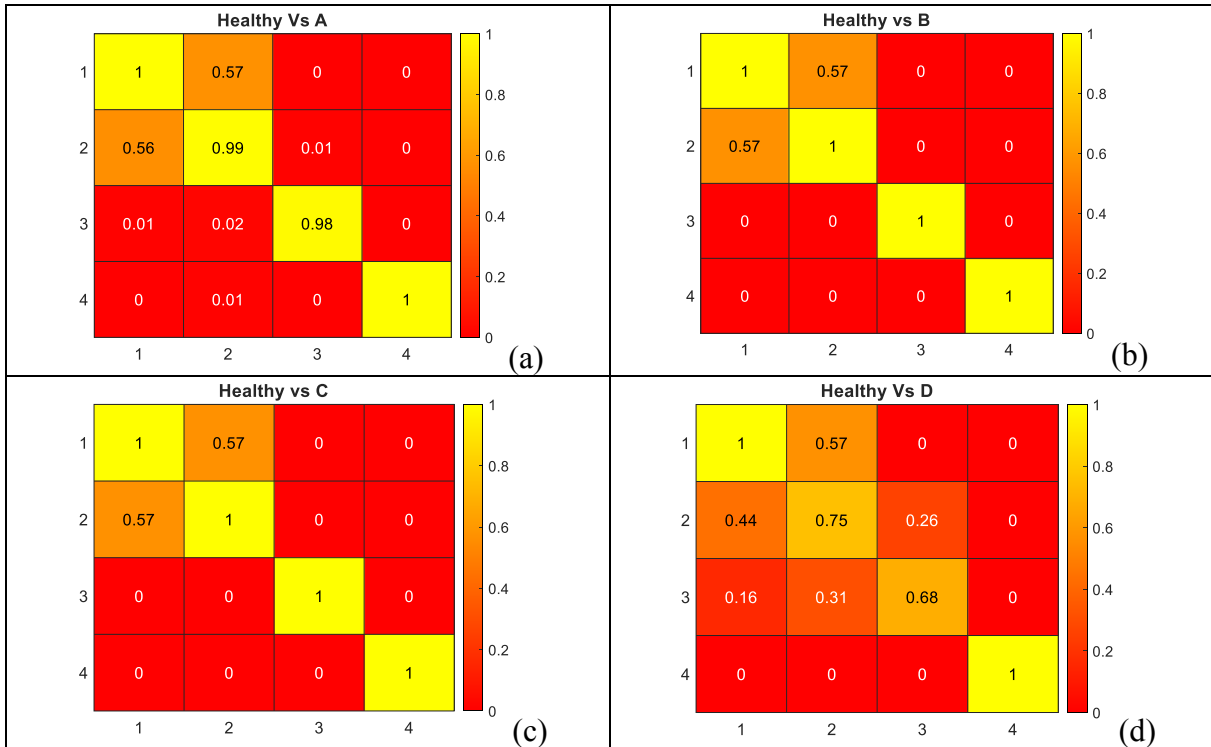


Figure 5: MAC matrices computed between healthy and damaged numerical mode shapes. (a): damage A. (b): damage B. (c): damage C. (d): damage D.

4 NON-MODAL BASED METHOD

This section deals with the direct usage of acceleration time series associated to train transit on the bridge, to compare healthy and damaged behavior. Three train's travelling speeds 100 km/h, 110 km/h and 120 km/h are investigated, corresponding to the real operating speeds. In addition, to take into consideration a more realistic scenario, the simulations were performed with ideal geometry of the track, and true measured geometrical track irregularity. Track geometrical irregularity, shown in Figure 6, was measured by the inspection train of the infrastructure manager, on the real bridge under investigation. Track geometrical irregularity is composed of three contributions, namely vertical level ($\sigma_v = 1.8 \text{ mm}$), lateral profile ($\sigma_y = 0.8 \text{ mm}$) and cross-elevation ($\sigma_r = 0.8 \text{ mm}$). It will be shown that track irregularity has a considerable masking effect on the capability of detect the presence of a damage. In the following the results for 120 km/h are reported, being very close for the other two speeds.

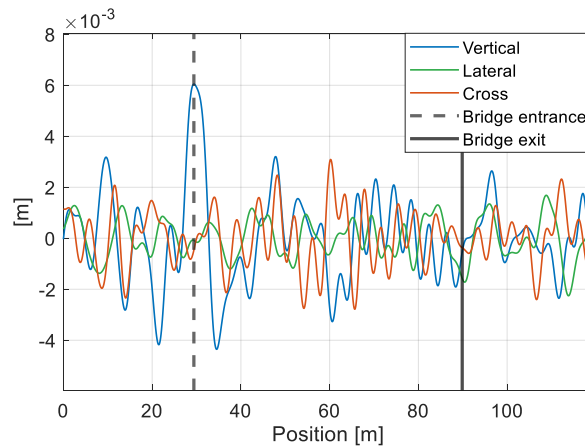


Figure 6: Track irregularity profile measured on the actual structure. Three contributions are considered, namely vertical, lateral and cross-elevation track geometries.

4.1 Results without track irregularity

This section aims to present the results obtained when no track irregularity is considered in the simulations, this correspond to an ideal condition and it is a comparison for the case in which track irregularity is considered. Damage scenario D is the only one that showed some sensitivity to damage the same outcome was obtained also referring to the study of bridge free motion following train transit.

The direct comparison between the two time series at points 3 and 4 in healthy and damaged scenario D is shown in Figure 7. The dynamical range is higher if track irregularity is included. The main impact of track irregularity is found from 4 Hz. The direct examination of the time series in Figure 7 shows some differences, a quantitative index is needed to summarize this difference.

To this purpose, the simulated acceleration outputs are first low-pass filtered at 20 Hz. A standard deviation analysis is then performed on a moving time window, with a length equal to the total travelling time divided by and integer n . The best performance was found with $n=3$. The window is continuously shifted with a time step equal to the time step of the output. In this way a smoothing effect is obtained, and the global differences induced by damage can be better revealed.

The moving standard deviation so defined, applied to the vertical acceleration output at nodes 1 to 6 is presented in Figure 8. Where it is possible to observe a difference between healthy and damaged clearer than the direct comparisons of the time series. To measure the distance between the curves, the ratio of the integral of the difference between the two curves and the integral of healthy curve is calculated. Maximum percentage is between 17 and 18%, for the central couple of points (N.3 and N.4).

The same analysis has been performed on the difference between left and right-hand side acceleration signals with the purpose to highlight the asymmetries introduced by the defect applied only on one side of the deck, in response to the passage of the rail vehicle, that is in centered position, above the longitudinal axis of the bridge. Figure 9 reports the obtained results: without track irregularity the only source of right-left asymmetry is the damage, so that its influence is strongly highlighted by this kind of analysis.

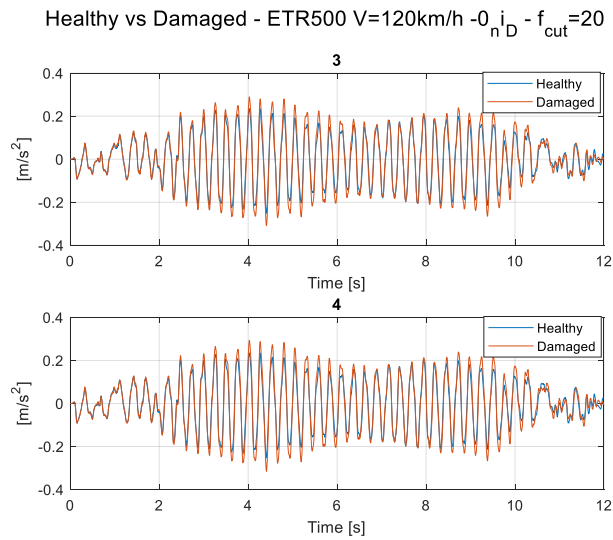


Figure 7: Vertical simulated acceleration at points 3 and 4 (see **Figure 1**) without track irregularity, in healthy and damaged condition.

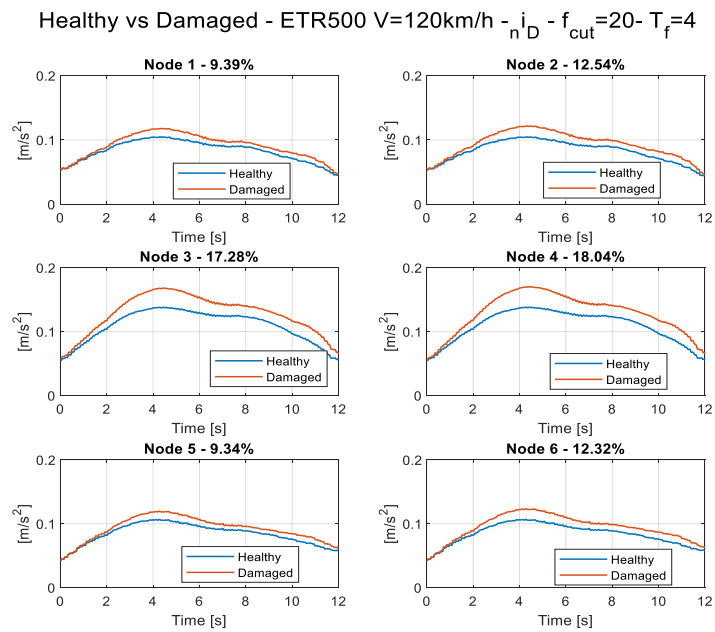


Figure 8: Moving standard deviation applied to the simulated acceleration time series obtained at points 1 to 6. ETR500 travelling at 120 km/h, without track irregularity.

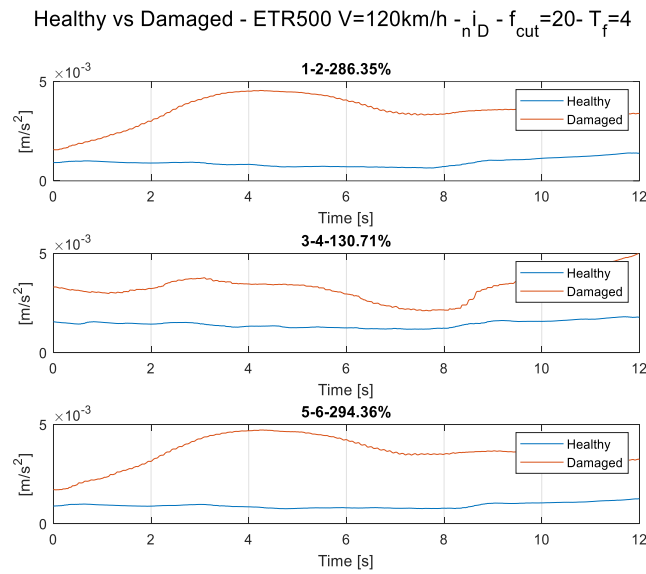


Figure 9: Moving standard deviation analysis applied to the right-left difference acceleration signals obtained at the three sections, considering ETR500 travelling at 100 km/h, no track irregularity.

4.2 Results in presence of track irregularity

The following step is represented by the consideration of track geometrical irregularity, with 100% measured level, and 33% of the measured level, to investigate the impact of this parameter on the capability to reveal the presence of the damage. Only scenario D is investigated, since for the others a clear indication could not be found. Figure 10 shows the simulated vertical acceleration in the same six points previously examined: now the peak level reaches 1 m/s^2 , against 0.3 m/s^2 (compare Figure 7 with Figure 10) without track irregularity.

The detection index (see Figure 11) has a similar trend maximum in the middle and decreasing with entrance and exit of the train, but now the difference is much lower, reduced to about 3%.

The standard deviation analysis on the difference between right and left side acceleration in correspondence of each section, was not significant, obtaining detection index around 11.5% only, so not applicable as robust index.

To quantify the influence of track irregularity, it was reduced to 33% of the original level, obtaining the results reported in Figure 12, where a considerable value of the detection index around 12% was obtained.

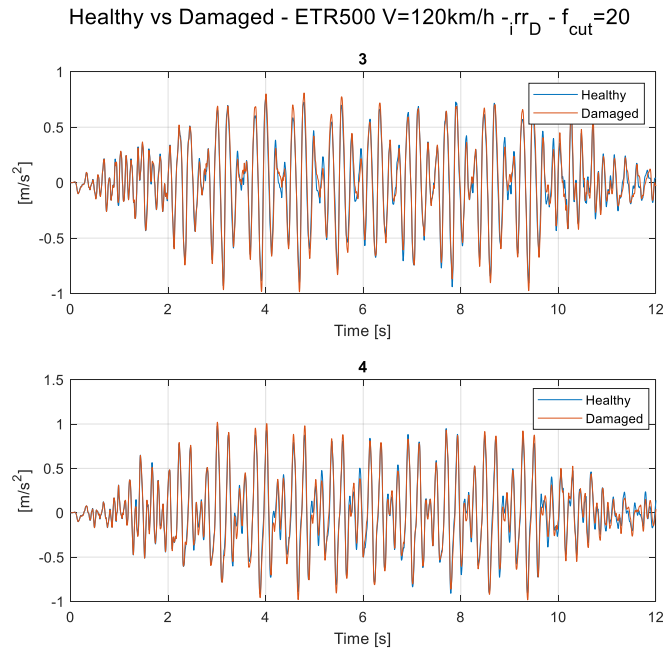


Figure 10: Vertical simulated acceleration at points 3 and 4 (see Figure 1) with 100% level track irregularity, in healthy and damaged condition.

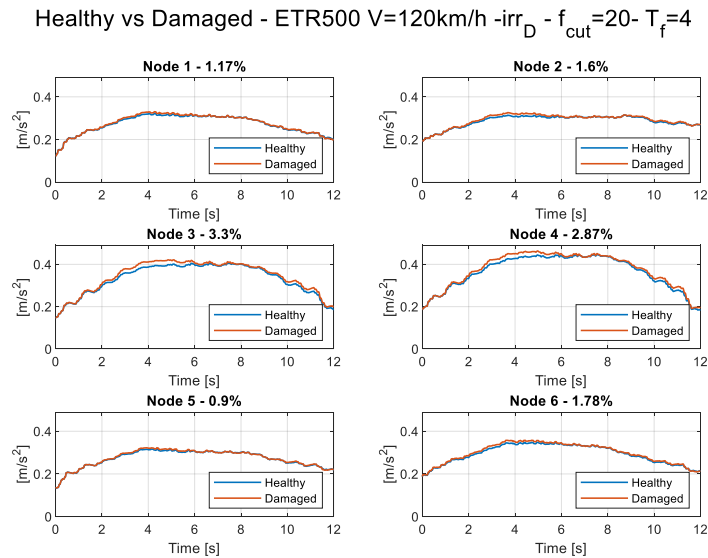


Figure 11: Moving standard deviation applied to the simulated acceleration time series obtained at points 1 to 6. ETR500 travelling at 120 km/h, with full level of track irregularity.

5 CONCLUSIONS

In this work, the authors investigated the possibility to reveal the presence of partial a damage in taking as an example an existing Warren truss bridge railway bridge, from time series acceleration analysis. The FEM model of the bridge was validated through natural frequencies and mode shapes comparison with the real bridge.

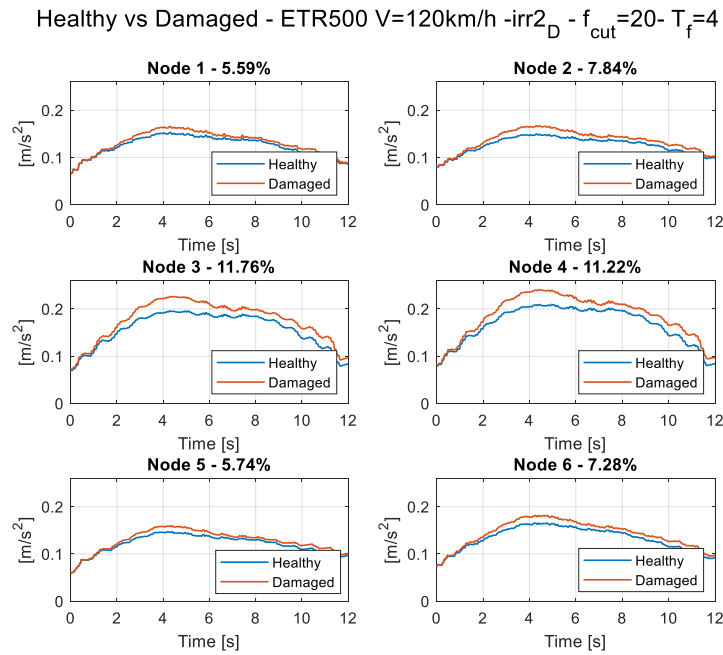


Figure 12: Moving standard deviation applied to the simulated acceleration time series obtained at points 1 to 6. ETR500 travelling at 120 km/h, with 33% level of track irregularity.

The validated bridge was then used to analyze the possibility to reveal the presence of a defect in some structural members of the bridge. The defect was implemented through a reduction at 50% of the Young modulus of a single structural member. The comparison between damaged and healthy condition of the bridge was carried out in two ways, namely frequency-based and time series-based approach.

Frequency-based approach: it consists in the analysis of the modification in the modal parameters (natural frequencies and mode shapes). Of the four considered damage scenarios, only one was clearly detectable, i.e., the one corresponding to a defect in the main lower chord on one side (damage scenario D), this was confirmed by frequencies shift and change in the MAC indexes of some of the modes.

Time series-based approach: the analysis is carried out on the acceleration in the time interval corresponding to train transit, processing the difference of acceleration in the two conditions, to extract a resuming index. To reduce the uncertainties related to the comparison of two time series, a reduction procedure has been implemented. Each time series (in damaged and healthy condition) is analyzed through a mobile rms window, in order too get a smoothing effect, but still retaining the difference of the signals power.

In this context an important element of the real scenario was introduce: the geometrical irregularity of the track, that plays the role of strong background disturbance, partially masking the difference in the acceleration between damaged and healthy condition. The detecting index reduces from 17% to 12% (with one third level of measured track irregularity and down to 3% for full level of measured track irregularity).

Further development of the research will focus on the application of data mining already applied in pass-by approach, to better extract a signature of the defect ([11]).

REFERENCES

- [1] A., Malekjafarian, P.J. McGentrick, E. J. Obrien. A review of Indirect Bridge Monitoring Using Passing Vehicles. *Shock and Vibration* 2015 (2015), 1-16, <https://doi.org/10.1155/2015/286139>.
- [2] Weiwei Lin, Rehabilitation and Strengthening of Aged Steel Railway Bridges in Japan, *Journal of Civil & Environmental Engineering*, 2018, 8:2, DOI: 10.4172/2165-784X.1000305
- [3] A. Dinas, Th.N. Nikolaidis, C.C. Baniotopoulos, Sustainable Restoration Criteria for a Historical Steel Railway Bridge, *International Conference on Sustainable Synergies from Buildings to the Urban Scale, SBE16, Procedia Environmental Sciences* 38 (2017) pp.578 – 585
- [4] D'Angelo, M.; Menghini, A.; Borlenghi, P.; Bernardini, L.; Benedetti, L.; Ballio, F.; Belloli, M.; Gentile C. Hydraulic Safety Evaluation and Dynamic Investigations of Baghetto Bridge in Italy. *Infrastructure* 2022, 7, 53. <https://doi.org/10.3390/infrastructures7040053>.
- [5] S. L. Davis and D. Goldberg, *The Fix We're In For: The State of Our Nation's Bridges 2013*, Transportation for America, Washington, DC, USA, 2013.
- [6] A. Znidaric, V. Pakrashi, E. O'Brien, and A. O'Connor, "A review of road structure data in six European countries", *Proceedings of the ICE: Urban Design and Planning*, vol. 164, no. 4, pp.225-232, 2011.
- [7] Chupanit P., Phromson C. (2012) The importance of bridge health monitoring. *International Science Index* 6: 135-138.
- [8] R. Helmerich, J. Bain, P. Cruz, A guideline for railway bridge inspection and condition assessment including the NDT toolbox, *Sustainable Bridges, - Assessment for Future Traffic Demands and Longer Lives*.
- [9] B. T. Svendsen, G. T. Frøseth, O. Øiseth¹, A. Rønnquist, A data-based structural health monitoring approach for damage detection in steel bridges using experimental data, *Journal of Civil Structural Health Monitoring* (2022) 12:101–115 <https://doi.org/10.1007/s13349-021-00530-8>
- [10] Meixedo A., Ribeiro D., Santos J., Calçada R., Todd M. Progressive numerical model validation of a bowstring-arch railway bridge based on a structural health monitoring system, *Journal of Civil Structural Health Monitoring*, Volume 11, Pages 421-449, 2021, 10.1007/s13349-020-00461-w.
- [11] Bernardini, L.; Carnevale, M.; Collina, A.; Identification in Warren Truss Bridges by Two Different Time-Frequency Algorithms. *Appl. Sci.* 2021, 11, x. <https://doi.org/10.3390/app112210605>
- [12] Swagato D., Saha P., Patro S. K. Vibration-based damage detection techniques used for health monitoring of structures: a review. *Journal of Civil Structural Health Monitoring*, Volume 6, Issue 3, Pages 477-507, 2016, 10.1007/s13349-016-0168-5.
- [13] Tee, Kong Fah, Time series for vibration-based structural health monitoring: A review, *SDHM Structural Durability and Health Monitoring*, Volume 12, Issue 3, Pages 129-147, 2018, 10.3970/sdhm.2018.04316.